# Universal Trade-Off between Power, Efficiency, and Constancy in Steady-State Heat Engines

Patrick Pietzonka and Udo Seifert
*II. Institut für Theoretische Physik, Universität Stuttgart, 70550 Stuttgart, Germany*

(Received 8 May 2017; revised manuscript received 12 December 2017; published 11 May 2018)

Heat engines should ideally have large power output, operate close to Carnot efficiency and show constancy, i.e., exhibit only small fluctuations in this output. For steady-state heat engines, driven by a constant temperature difference between the two heat baths, we prove that out of these three requirements only two are compatible. Constancy enters quantitatively the conventional trade-off between power and efficiency. Thus, we rationalize and unify recent suggestions for overcoming this simple trade-off. Our universal bound is illustrated for a paradigmatic model of a quantum dot solar cell and for a Brownian gyrator delivering mechanical work against an external force.

DOI: 10.1103/PhysRevLett.120.190602

The efficiency $\eta$ of heat engines operating cyclically between a hot heat reservoir at temperature $T_h$ and a cold one at $T_c$ is universally bounded from above by the Carnot value $\eta_C \equiv 1 - T_c/T_h$. Moreover, it was commonly believed that reaching Carnot efficiency inevitably comes with a vanishing power $P$ since such engines require quasistatic conditions leading to an infinite cycle-time. This supposedly universal trade-off between power and efficiency has more recently been challenged by studies hinting at the possibility to come at least arbitrarily close to Carnot efficiency with finite power by a particular coupling between subsystems [1] or by exploiting a working substance at a critical point [2]. On the other hand, a general bound of the type $P \leq A(\eta_C - \eta)$ with a system-specific amplitude $A$ has been proven for cyclic engines both in linear response [3] and beyond [4]. These two strands of reasoning can be reconciled only if one allows for a diverging amplitude $A$ as the efficiency approaches the Carnot value.

For steady-state heat engines permanently coupled to two heat baths like in thermoelectric setups, the common argument from above invoking quasistatic conditions and hence an infinite cycle time is not directly applicable. It has usually been replaced with the idea that finite currents necessarily lead to dissipation which should spoil the option of reaching the Carnot limit at finite power. This view was challenged by a seminal paper from Benenti *et al.* [5], who pointed out that if time-reversal symmetry is broken, like in the presence of a magnetic field, the usual approach based on linear irreversible thermodynamics does not forbid Carnot efficiency at finite power. Subsequent studies showed with somewhat more specific assumptions that Carnot efficiency at finite power is not accessible. This holds true, e.g., for any finite number of terminals in a multiterminal set-up within linear response theory [6,7], and for an effective two-terminal device containing inelastic electron-phonon processes [8]. However, as for cyclic engines, it has recently been pointed out that in certain limits Carnot efficiency at finite power can be reached in models of steady-state engines. Specific proposals include two-cycle engines with diverging affinities [9], a specially designed Feynman-Smoluchowski ratchet [10], and systems with a singular transport law [11,12].

These observations taken together indicate that when searching for a universal trade-off it may not be enough to focus only on the *two* characteristics power and efficiency, and their relationship if one of them becomes maximal as it is typically done, see also [13–28]. As we will show in this Letter, as a crucial *third* quantity, power fluctuations enter quantitatively into this balance. Specifically, we will prove for a huge class of steady-state heat engines, which includes all thermodynamically consistent machines with a classical discrete set of internal states and continuous ones modeled with an overdamped Langevin dynamics, that there is a universal trade-off between three desiderata: Finite (or even large) power, an efficiency close to the Carnot value, and constancy in the sense of small fluctuations in the power output are not compatible. Specifically, the bound

$$P \frac{\eta}{\eta_C - \eta} \frac{T_c}{\Delta_P} \leq \frac{1}{2} \tag{1}$$

constrains (mean) output power, efficiency, and the power fluctuations in finite time as measured by

$$\Delta_P \equiv \lim_{t\to\infty} \langle (P(t) - P)^2 \rangle t. \tag{2}$$

Here, $P(t)$ is the fluctuating power after time $t$ evaluated in the steady state, for which $\langle \ldots \rangle$ denotes averages. Since the

 © 2018 American Physical Society

mean output work grows linearly in time as does its variance, converting work fluctuations into power fluctuations requires the additional factor of $t$ to reach a finite limit for $\Delta_P$, with which we characterize the constancy, or stability [29], of the engine. In particular for nanoscopic heat engines, power fluctuations due to thermal noise are not negligible compared to the mean work output on relevant time scales and should therefore be taken into account for a thermodynamic description. The crucial role power fluctuations play in the above bound is complementary to their effect in the statistics of efficiency in a finite time [30–33].

As a main first consequence of this new bound for steady-state heat engines, it is obvious that as long as the power fluctuations remain finite (and $T_c$ as well), approaching Carnot efficiency implies that the power has to vanish at least linearly. The explicit occurrence of $\Delta_P$ as an amplitude in a putative linear relationship between power and efficiency gap to Carnot, however, offers a second option. If the fluctuations blow up, then a finite (or even diverging) power is not ruled out as $\eta \to \eta_C$, which unifies quantitatively the various observations recalled above.

The bound (1) can be rearranged as a bound on efficiency

$$\eta \leq \frac{\eta_C}{1 + 2PT_c/\Delta_P}, \tag{3}$$

determined by mean and fluctuations of the output power. Thus, the efficiency of any steady-state heat engine is bounded from above by this simple expression independent of the specific design of the engine. The formal similarity of (3) with a bound derived for the efficiency of molecular motors [34] indicates as common origin of these bounds the thermodynamic uncertainty relation [35,36], which describes a universal inequality between entropy production and mean and variance of an arbitrary current.

For a proof of the universal trade-off (1), we consider an engine characterized by a set of internal states $\{i\}$ with internal energies $\{E_i\}$. A transition between state $i$ and $j$ takes place with a rate $k_{ij}^c$ if it is mediated by the contact to the cold bath and with a rate $k_{ij}^h$ if it is mediated by the hot bath. One of these rates can be zero, which means that this particular transition always involves the other bath. For any nonzero rate, the corresponding backward rate does not vanish either, and it obeys the local detailed balance condition [37]

$$\frac{k_{ij}^{c,h}}{k_{ji}^{c,h}} = \exp[(E_i - E_j + b_{ij}^{c,h}\mu_{c,h} - f d_{ij})/T_{c,h}], \tag{4}$$

where we set Boltzmann's constant to 1 throughout the Letter. Here, $E_{i,j}$ are the internal energies of the two states. If the transition from $i$ to $j$ requires the transport of an electron from the bath with temperature $T_a$ $(a = c, h)$ and chemical potential $\mu_a$ to the system, then $b_{ij}^a = 1$. Likewise, if this transition involves the release of an electron to a bath, $b_{ij}^a = -1$. In both cases, the chemical potentials enter the expression in the exponent providing a contribution to the total free energy involved in such a transition. The last term in the exponent is nonzero if this transition additionally involves a step of length $d_{ij}$ against an external force $f$. Generalizations to several species of particles, further baths, or the case of rotary motion against an applied torque should be obvious.

In the steady state, where state $i$ is realized with probability $p_i$, this engine can be characterized by three important mean currents, the heat current

$$j_h = \sum_{i<j} (p_i k_{ij}^h - p_j k_{ji}^h)(E_j - E_i - b_{ij}^h \mu_h) \tag{5}$$

from the hot bath to the engine, the heat current

$$j_c = -\sum_{i<j} (p_i k_{ij}^c - p_j k_{ji}^c)(E_j - E_i - b_{ij}^c \mu_c) \tag{6}$$

from the engine to the cold bath, and the "work current"

$$j_w = j_h - j_c = P, \tag{7}$$

which, due to the first law, is the power delivered by the engine. Running the engine for a finite time $t$, each of the currents will fluctuate around these mean values with a dispersion [38]

$$D_\alpha \equiv \lim_{t\to\infty} \langle (j_\alpha(t) - j_\alpha)^2 \rangle t/2, \tag{8}$$

where $\alpha = h,\ c,\ w$. The mean entropy production rate becomes

$$\sigma = j_c/T_c - j_h/T_h = j_w(\eta_C/\eta - 1)/T_c. \tag{9}$$

Since this Markovian network is thermodynamically consistent, one can directly apply the thermodynamic uncertainty relation, which reads for any of the three currents [35,36]

$$\sigma D_\alpha \geq j_\alpha^2. \tag{10}$$

Evaluating this relation for the work current, $\alpha = w$, leads, with $\Delta_P = 2D_w$, (7) and (9), to the bound (1).

Two related, but not identical, forms of this bound can be derived similarly by applying the thermodynamic uncertainty relation to either the heat current from the hot bath or the one entering the cold bath. Expressed as bound on power, they read explicitly

$$P \leq (\eta_C - \eta)\eta D_h/T_c \tag{11}$$

and

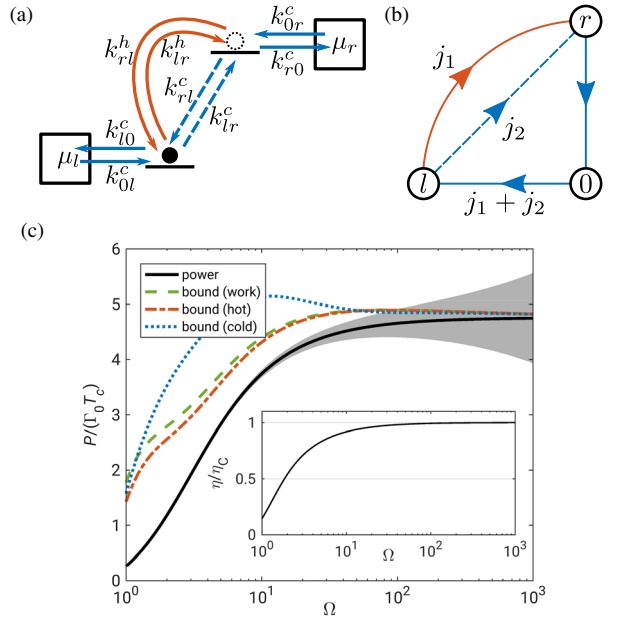


FIG. 1. (a) Model for a photoelectric device, transporting electrons between two reservoirs through a quantum dot with two energy levels. Transitions to and from the baths (blue solid arrows) and nonradiative transitions between the energy levels (blue dashed arrows) occur in contact with the cold bath. Radiative transitions (red curved arrows) occur in contact with the hot bath. (b) The network representation of the three possible states of the quantum dot allows for an identification of the two cycle currents associated with radiative ($j_1$) and nonradiative transitions ($j_2$). (c) Output power and efficiency (inset) of the photoelectric device as a function of the scaling parameter $\Omega$ entering the rates and affinities according to $x_c = 10$, $x_h = 0.2$, $x_l = 1$, $x_r = 1.2 + 7/\Omega$, $\Gamma_l = \Gamma_r = \Gamma_h = \Omega\Gamma_0$, $\Gamma_c = \Omega^{-1.5}\Gamma_0$, where $\Gamma_0$ is a frequency of reference. The power fluctuations, quantified by $\sqrt{\Delta_P/(10\Gamma_0)}$, are shown as a grey shaded region. The three bounds on the output power (1), (11), (12) are shown as dashed, dash-dotted and dotted curves, respectively.

$$P \leq (\eta_C - \eta)\eta D_c/[(1-\eta)^2 T_c], \tag{12}$$

respectively. Obviously, in order to reach a finite value for the power as $\eta \to \eta_C$, the fluctuations in all three currents have to diverge at least $\sim 1/(\eta_C - \eta)$ since each of the three bounds (1), (11), (12) has to be respected.

For an illustration of these bounds, we consider a simple but instructive model for a solar cell introduced in Ref. [39] as shown in Fig. 1(a). It consists of a two level quantum dot that can either be empty (state 0) or contain an electron in one of the levels $E_l < E_r$ (states $l$ and $r$, respectively). Electrons are transported through the dot from a left reservoir with chemical potential $\mu_l$ and temperature $T_c$ to a right reservoir with higher chemical potential $\mu_r$ and the same temperature $T_c$. They enter the level $E_l$ from the left reservoir at a rate $k^c_{0l}$, and they jump back at a rate $k^c_{l0}$. Analogously, the level $E_r$ is connected to the right reservoir via the transition rates $k^c_{r0}$ and $k^c_{0r}$. Transitions between the two states can occur either nonradiatively through interactions with the surrounding phonon bath at temperature $T_c$ with rates $k^c_{lr}$ and $k^c_{rl}$ or are mediated by the black body radiation of the sun with temperature $T_h$ at rates $k^h_{lr}$ and $k^h_{rl}$. The transition rates to and from the two electron reservoirs ($i = l, r$) are chosen according to the Fermi-Dirac distribution as

$$k^c_{0i} = \Gamma_i/[1+\exp(x_i)], \quad k^c_{i0} = \Gamma_i/[1+\exp(-x_i)] \tag{13}$$

with frequencies $\Gamma_i$ and affinities $x_i = (E_i - \mu_i)/T_c$. The transition rates between the two states in contact with the cold phonon bath or hot photon bath ($a = c, h$, respectively) are determined by the Bose-Einstein distribution

$$k^a_{lr} = \Gamma_a/[\exp(x_a) - 1], \quad k^a_{rl} = \Gamma_a/[1-\exp(-x_a)], \tag{14}$$

with frequencies $\Gamma_j$ and affinities $x_a = (E_r - E_l)/T_a$. All four pairs of rates satisfy the local detailed balance condition (4).

In a network representation of this system [Fig. 1(b)], we can identify two independent cycle currents. The variables $X_1$ and $X_2$ count the net number of electrons transported from state $l$ to state $r$ via radiative and nonradiative transitions, respectively. The total number of transported electrons is thus $X_e = X_1 + X_2$ (up to a single electron that might still be in the two-level system, which does not affect the statistics of fluctuations in the long-time limit). The joint fluctuations of these counting variables are characterized by the average currents $\langle X_{1,2}(t)\rangle = j_{1,2}t$ and their covariance $\langle (X_i(t) - j_i t)(X_j(t) - j_j t)\rangle = 2D_{ij}t$ for large $t$, which can be calculated directly from the rates (13) and (14) [40].

For the mean power, mean heat current from the hot reservoir, and mean heat current into the cold reservoir, one obtains

$$P = \Delta\mu(j_1 + j_2), \tag{15}$$

$$j_h = \Delta E j_1, \tag{16}$$

$$j_c = (\Delta E - \Delta\mu)j_1 - \Delta\mu j_2, \tag{17}$$

respectively, with $\Delta E \equiv E_r - E_l$ and $\Delta\mu \equiv \mu_r - \mu_l$. For the corresponding dispersion coefficients, one gets

$$D_w = \Delta\mu^2(D_{11} + D_{22} + 2D_{12}), \tag{18}$$

$$D_h = \Delta E^2 D_{11}, \tag{19}$$

$$D_c = (\Delta E - \Delta\mu)^2 D_{11} + \Delta\mu^2 D_{22} - 2(\Delta E - \Delta\mu)\Delta\mu D_{12}. \tag{20}$$

In the "strong coupling" limit of negligible nonradiative transitions ($\Gamma_c \to 0$ and hence $X_2$, $j_2$, $D_{22}$, and $D_{12} \to 0$),

the efficiency of the photoelectric device becomes $\eta = \Delta\mu/\Delta E$. By gradually increasing the chemical potential difference $\Delta\mu$ with fixed $\Delta E$, this ratio can approach $\eta_C$ from below. In Fig. 1(c), this limit is realized by increasing the chemical potential $\mu_r$ via a scaling parameter $\Omega$ while keeping $\mu_l$, the energies, and the temperatures fixed, as detailed in the caption. We show that finite power can be achieved in this limit by increasing the rates $\Gamma_l$, $\Gamma_r$, and $\Gamma_h$ while reducing $\Gamma_c$ [44]. Crucially, as predicted by relation (1), the fluctuations of the output power diverge in such a scenario.

The uncertainty relation (10) becomes tight in the linear response limit for unicyclic networks [35]. Hence, for strong coupling and vanishing cycle affinity

$$\ln \frac{k_{0l}^c k_{lr}^h k_{r0}^c}{k_{0r}^c k_{rl}^h k_{l0}^c} = x_r - x_l - x_h = (\eta_C \Delta E - \Delta\mu)/T_c, \qquad (21)$$

as realized for a large scaling parameter $\Omega$ in Fig. 1(c), all three bounds on the power output (1), (11), (12) saturate. Beyond the linear response and strong-coupling limit, the bounds can become weaker. As explored in the Supplemental Material [40], depending on the values of the transition frequencies, each of the three bounds can become the strongest one, demonstrating that these are independent bounds.

Since the thermodynamic uncertainty relation (10) has also been proven for overdamped Langevin dynamics [45,46], the resulting trade-offs apply as well to steady-state heat engines modeled on such a continuous state space. For an analytically solvable illustration, we consider the so-called Brownian gyrator [47], which has recently been realized experimentally in an electronic [48] and in a colloidal system [49]. The setup, shown in Fig. 2(a), consists of a point particle with mobility $\mu$ in two dimensions and an anisotropic harmonic potential $V(\boldsymbol{x}) = (u_1 x_1^2 + u_2 x_2^2)/2 + c x_1 x_2$ with $u_{1,2} > 0$ and $0 < c < \sqrt{u_1 u_2}$. Its motion obeys the Langevin equation

$$d\boldsymbol{x}/dt = \mu[-\partial V/\partial \boldsymbol{x} + \boldsymbol{F}^{\mathrm{ext}}(\boldsymbol{x})] + \boldsymbol{\zeta}(t), \qquad (22)$$

where the noise term has mean $\langle \boldsymbol{\zeta}(t) \rangle = 0$ and correlations $\langle \zeta_i(t)\zeta_j(t') \rangle = 2\mu T_i \delta_{ij}\delta(t-t')$; i.e., the two components of the fluctuating force are associated with heat reservoirs at two different temperatures $T_i$. We choose $T_1 \equiv T_c < T_2 \equiv T_h$. In the established case with $\boldsymbol{F}^{\mathrm{ext}}(\boldsymbol{x}) = 0$, the coupling $c \neq 0$ in the potential mediates a steady transfer of heat from the hot to the cold reservoir, that is accompanied by a persistent directed gyration of the particle [47]. In order to extract mechanical work from this gyration, we load the engine with a nonconservative external counter force $\boldsymbol{F}^{\mathrm{ext}}(\boldsymbol{x})$. As the simplest, linear realization of such a force, we choose $\boldsymbol{F}^{\mathrm{ext}}(\boldsymbol{x}) = (F_1^{\mathrm{ext}}, F_2^{\mathrm{ext}})^T = k(x_2, -x_1)^T$ with a parameter $k$. Following the rules of stochastic

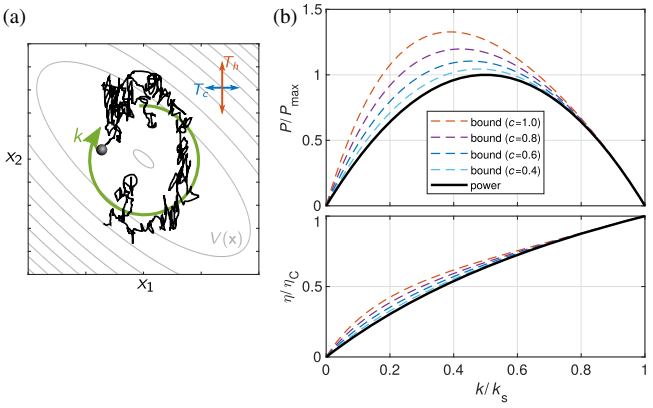


FIG. 2. (a) Schematic trajectory of a Brownian gyrator with the two-dimensional potential $V(x_1, x_2)$ shown as contour lines. The anisotropic noise leads to a gyration in counter-clockwise direction against the external force with parameter $k$. (b) Scaled power (top) and efficiency (bottom) as a function of the force parameter $k$. The respective bounds (11) and (3) become tighter with decreasing $c$. Parameters: $T_c = 1$, $T_h = 7$, $\mu = 1$, $u_1 = 1$, $u_2 = 1.2$.

thermodynamics [37], along an individual trajectory we identify the work

$$đw = -d\boldsymbol{x} \cdot \boldsymbol{F}^{\mathrm{ext}}(\boldsymbol{x}), \qquad (23)$$

performed against the external force, the heat

$$đq_c = dx_1[-\partial V(\boldsymbol{x})/\partial x_1 + F_1^{\mathrm{ext}}(\boldsymbol{x})] \qquad (24)$$

dissipated into the cold heat bath, and the heat

$$đq_h = -dx_2[-\partial V(\boldsymbol{x})/\partial x_2 + F_2^{\mathrm{ext}}(\boldsymbol{x})] \qquad (25)$$

extracted from the hot heat bath. The corresponding integrated currents follow from these differentials through the Stratonovich integration scheme.

The average mechanical power can be calculated as [40]

$$P = j_w = \langle đw/dt \rangle = 4P_{\max}\frac{k}{k_s}\left(1 - \frac{k}{k_s}\right), \qquad (26)$$

with the stall parameter $k_s \equiv c\eta_C/(2-\eta_C)$ and the maximal power $P_{\max} \equiv \mu k_s^2 (T_c + T_h)/(2(u_1 + u_2))$. The system operates as a heat engine, delivering mechanical work for $0 < k < k_s$. Its efficiency is then given by

$$\eta = j_w/j_h = 2k/(c+k) \leq \eta_C. \qquad (27)$$

The diffusion coefficients $D_{w,c,h}$ of the three currents can be calculated analytically as well. It turns out that the uncertainty relation (10) becomes the same for each current,

$$\frac{D_w\sigma}{j_w^2}=\frac{D_c\sigma}{j_c^2}=\frac{D_h\sigma}{j_h^2}=1+\frac{[c\eta_C(1-k/k_s)]^2}{(u_1+u_2)^2(1-\eta_C)}\geq 1, \quad (28)$$

with the entropy production rate $\sigma$ as defined in Eq. (9). The resulting bounds on the power and efficiency are shown in Fig. 2(b). These bounds become strong when the ratio $D_w\sigma/j_w^2$ in Eq. (28) is close to one, as it is the case for moderate temperature differences or small couplings $c$ with respect to the parameters $u_{1,2}$. For $k$ close to $k_s$, the bounds on both power and efficiency become tight in linear order in $(k_s-k)$, independently of all other parameters. Because of a tight coupling between heat and work currents, this regime corresponds to a weak driving of the system within linear response, for which the uncertainty relation can generally be saturated. For $k\to k_s$, as the efficiency approaches the Carnot limit, the power vanishes. Since the constancy of the power remains finite, this typical behavior of a heat engine can be interpreted as a consequence of the universal relation (1). The unusual case of finite power close to Carnot efficiency can yet be obtained by scaling the mobility $\mu$, which comes at the cost of diverging power fluctuations [40].

In summary, we have derived a bound providing a universal trade-off between power, efficiency, and constancy, i.e., fluctuations in the power output. A finite (or even diverging) power as Carnot efficiency is approached, necessarily requires the latter to diverge. The three versions of the bound hold beyond the linear response regime of a small temperature difference between the two heat reservoirs. We have derived these results for steady-state engines described by thermodynamically consistent Markovian dynamics on a discrete state space and for overdamped Langevin dynamics. They also apply to apparently non-Markovian heat engines, provided that there is a sufficiently fine-grained level of description on which the system obeys Markovian stochastic dynamics, however complex this description might be. The generalization to underdamped Langevin dynamics might be somewhat more subtle.

One might expect that similar results could be derived for cyclic, i.e., periodically driven, heat engines [15] that can be experimentally realized for colloidal systems [50,51] and with active baths [52]. In particular, a certain formal analogy of (1) with the bound derived in [4] for cyclic engines is striking. However, the analysis of a periodically driven Brownian clock in [53] shows that the steady-state bound (10), relating entropy production, mean current, and dispersion, cannot naively be extended to periodically driven systems. Therefore, it remains an exciting open question whether there are periodically driven heat engines that beat the, for steady-state engines universal, bound (1).

We have focused on the question whether Carnot efficiency can be reached with finite power. More generally, one can ask for any given class of machines whether the power at the maximal efficiency, which may be less than Carnot (or less than 1 for isothermal machines), can be bounded or shown to vanish. Exploring this issue, using the techniques introduced here, will be left to future work. Finally, it will be interesting to investigate whether and how constancy enters bounds for genuine quantum heat engines that exploit coherences—see [54] and references therein.


[1] A. E. Allahverdyan, K. V. Hovhannisyan, A. V. Melkikh, and S. G. Gevorkian, Carnot Cycle at Finite Power: Attainability of Maximal Efficiency, Phys. Rev. Lett. **111**, 050601 (2013).

[2] M. Campisi and R. Fazio, The power of a critical heat engine, Nat. Commun. **7**, 11895 (2016).

[3] K. Brandner, K. Saito, and U. Seifert, Thermodynamics of Micro- and Nano-Systems Driven by Periodic Temperature Variations, Phys. Rev. X **5**, 031019 (2015).

[4] N. Shiraishi, K. Saito, and H. Tasaki, Universal Trade-Off Relation between Power and Efficiency for Heat Engines, Phys. Rev. Lett. **117**, 190601 (2016).

[5] G. Benenti, K. Saito, and G. Casati, Thermodynamic Bounds on Efficiency for Systems with Broken Time-Reversal Symmetry, Phys. Rev. Lett. **106**, 230602 (2011).

[6] K. Brandner and U. Seifert, Multi-terminal thermoelectric transport in a magnetic field: Bounds on Onsager coefficients and efficiency, New J. Phys. **15**, 105003 (2013).

[7] K. Brandner and U. Seifert, Bound on thermoelectric power in a magnetic field within linear response, Phys. Rev. E **91**, 012121 (2015).

[8] K. Yamamoto, O. Entin-Wohlman, A. Aharony, and N. Hatano, Efficiency bounds on thermoelectric transport in magnetic fields: The role of inelastic processes, Phys. Rev. B **94**, 121402 (2016).

[9] M. Polettini and M. Esposito, Carnot efficiency at divergent power output, Europhys. Lett. **118**, 40003 (2017).

[10] J. S. Lee and H. Park, Carnot efficiency is reachable in an irreversible process, Sci. Rep. **7**, 10725 (2017).

[11] N. Shiraishi, Attainability of Carnot efficiency with autonomous engines, Phys. Rev. E **92**, 050101 (2015).

[12] J. Koning and J. O. Indekeu, Engines with ideal efficiency and nonzero power for sublinear transport laws, Eur. Phys. J. B **89**, 248 (2016).

[13] F. L. Curzon and B. Ahlborn, Efficiency of a Carnot engine at maximum power output, Am. J. Phys. **43**, 22 (1975).

[14] C. Van den Broeck, Thermodynamic Efficiency at Maximum Power, Phys. Rev. Lett. **95**, 190602 (2005).

[15] T. Schmiedl and U. Seifert, Efficiency at maximum power: An analytically solvable model for stochastic heat engines, Europhys. Lett. **81**, 20003 (2008).

[16] Z. C. Tu, Efficiency at maximum power of Feynman's ratchet as a heat engine, J. Phys. A **41**, 312003 (2008).

[17] M. Esposito, K. Lindenberg, and C. Van den Broeck, Universality of Efficiency at Maximum Power, Phys. Rev. Lett. **102**, 130602 (2009).

[18] N. Nakpathomkun, H. Q. Xu, and H. Linke, Thermoelectric efficiency at maximum power in low-dimensional systems, Phys. Rev. B **82**, 235428 (2010).

[19] U. Seifert, Efficiency of Autonomous Soft Nano-Machines at Maximum Power, Phys. Rev. Lett. **106**, 020601 (2011).

[20] Y. Izumida and K. Okuda, Efficiency at maximal power of minimal nonlinear irreversible heat engines, Europhys. Lett. **97**, 10004 (2012).

[21] N. Golubeva and A. Imparato, Efficiency at Maximum Power of Interacting Molecular Machines, Phys. Rev. Lett. **109**, 190602 (2012).

[22] C. de Tomas, J. M. M. Roco, A. C. Hernández, Y. Wang, and Z. C. Tu, Low-dissipation heat devices: Unified trade-off optimization and bounds, Phys. Rev. E **87**, 012105 (2013).

[23] J. Stark, K. Brandner, K. Saito, and U. Seifert, Classical Nernst Engine, Phys. Rev. Lett. **112**, 140601 (2014).

[24] R. S. Whitney, Most efficient Quantum Thermoelectric at Finite Power Output, Phys. Rev. Lett. **112**, 130601 (2014).

[25] J.-H. Jiang, Thermodynamic bounds and general properties of optimal efficiency and power in linear responses, Phys. Rev. E **90**, 042126 (2014).

[26] O. Raz, Y. Subaşı, and R. Pugatch, Geometric Heat Engines Featuring Power that Grows with Efficiency, Phys. Rev. Lett. **116**, 160601 (2016).

[27] M. Bauer, K. Brandner, and U. Seifert, Optimal performance of periodically driven, stochastic heat engines under limited control, Phys. Rev. E **93**, 042112 (2016).

[28] K. Proesmans, B. Cleuren, and C. Van den Broeck, Power-Efficiency-Dissipation Relations in Linear Thermodynamics, Phys. Rev. Lett. **116**, 220601 (2016).

[29] V. Holubec, An exactly solvable model of a stochastic heat engine: optimization of power, power fluctuations and efficiency, J. Stat. Mech. (2014) P05022; V. Holubec and A. Ryabov, Work and power fluctuations in a critical heat engine, Phys. Rev. E **96**, 030102(R) (2017).

[30] G. Verley, M. Esposito, T. Willaert, and C. Van den Broeck, The unlikely Carnot efficiency, Nat. Commun. **5**, 4721 (2014).

[31] T. R. Gingrich, G. M. Rotskoff, S. Vaikuntanathan, and P. L. Geissler, Efficiency and large deviations in time-asymmetric stochastic heat engines, New J. Phys. **16**, 102003 (2014).

[32] M. Polettini, G. Verley, and M. Esposito, Efficiency Statistics at All Times: Carnot Limit at Finite Power, Phys. Rev. Lett. **114**, 050601 (2015).

[33] K. Proesmans and C. Van den Broeck, Stochastic efficiency: five case studies, New J. Phys. **17**, 065004 (2015).

[34] P. Pietzonka, A. C. Barato, and U. Seifert, Universal bound on the efficiency of molecular motors, J. Stat. Mech. (2016) 124004.

[35] A. C. Barato and U. Seifert, Thermodynamic Uncertainty Relation for Biomolecular Processes, Phys. Rev. Lett. **114**, 158101 (2015).

[36] T. R. Gingrich, J. M. Horowitz, N. Perunov, and J. L. England, Dissipation Bounds All Steady-State Current Fluctuations, Phys. Rev. Lett. **116**, 120601 (2016).

[37] U. Seifert, Stochastic thermodynamics, fluctuation theorems, and molecular machines, Rep. Prog. Phys. **75**, 126001 (2012).

[38] The fluctuating currents $j_\alpha(t)$ are formally defined as $j_h(t)=\sum_{i<j} n^h_{ij}(t)(E_j-E_i-b^h_{ij}\mu_h)/t$, $j_c(t)=-\sum_{i<j} n^c_{ij}(t)\times(E_j-E_i-b^c_{ij}\mu_c)/t$, and $j_w(t)=\sum_{i<j}[-b^h_{ij}n^h_{ij}(t)(\mu_h-\mu_c)+(n^h_{ij}(t)+n^c_{ij}(t))fd_{ij}]/t$, with $n^a_{ij}(t)$ being the net number of transitions between $i$ and $j$, mediated by the hot ($a=h$) or cold ($a=c$) bath up to the time $t$.

[39] B. Rutten, M. Esposito, and B. Cleuren, Reaching optimal efficiencies using nanosized photoelectric devices, Phys. Rev. B **80**, 235122 (2009).

[40] See Supplemental Material (including Refs. [41–43]) at http://link.aps.org/supplemental/10.1103/PhysRevLett.120.190602 for detailed calculations for the quantum dot solar cell and the Brownian gyrator.

[41] Z. Koza, General technique of calculating the drift velocity and diffusion coefficient in arbitrary periodic systems, J. Phys. A **32**, 7637 (1999).

[42] M. Baiesi, C. Maes, and K. Netočný, Computation of current cumulants for small nonequilibrium systems, J. Stat. Phys. **135**, 57 (2009).

[43] H. Touchette, Introduction to dynamical large deviations of Markov processes, Physica (Amsterdam) **A**, DOI: 10.1016/j.physa.2017.10.046, 2018.

[44] A similar scaling has been used to achieve Carnot efficiency at divergent power output in Ref. [9].

[45] M. Polettini, A. Lazarescu, and M. Esposito, Tightening the uncertainty principle for stochastic currents, Phys. Rev. E **94**, 052104 (2016).

[46] T. R. Gingrich, G. M. Rotskoff, and J. M. Horowitz, Inferring dissipation from current fluctuations, J. Phys. A **50**, 184004 (2017).

[47] R. Filliger and P. Reimann, Brownian gyrator: A Minimal Heat Engine on the Nanoscale, Phys. Rev. Lett. **99**, 230602 (2007).

[48] K.-H. Chiang, C.-L. Lee, P.-Y. Lai, and Y.-F. Chen, Electrical autonomous Brownian gyrator, Phys. Rev. E **96**, 032123 (2017).

[49] A. Argun, J. Soni, L. Dabelow, S. Bo, G. Pesce, R. Eichhorn, and G. Volpe, Experimental realization of a minimal microscopic heat engine, Phys. Rev. E **96**, 052106 (2017).

[50] V. Blickle and C. Bechinger, Realization of a micrometre-sized stochastic heat engine, Nat. Phys. **8**, 143 (2012).

[51] I. A. Martínez, E. Roldán, L. Dinis, D. Petrov, J. M. R. Parrondo, and R. A. Rica, Brownian Carnot engine, Nat. Phys. **12**, 67 (2016).

[52] S. Krishnamurthy, S. Ghosh, D. Chatterji, R. Ganapathy, and A. K. Sood, A micrometre-sized heat engine operating between bacterial reservoirs, Nat. Phys. **12**, 1134 (2016).

[53] A. C. Barato and U. Seifert, Cost and Precision of Brownian Clocks, Phys. Rev. X **6**, 041053 (2016).

[54] K. Brandner, M. Bauer, and U. Seifert, Universal Coherence-Induced Power Losses of Quantum Heat Engines in Linear Response, Phys. Rev. Lett. **119**, 170602 (2017).